

RESEARCH PAPER



MiR-4268 suppresses gastric cancer genesis through inhibiting keratin 80

Fan Zhang^{a, #}, Guoxian Wang^{b, #}, Wenjuan Yan^c, and Hongmei Jiang^d

^aDepartment of Gastroenterology, Puren Hospital Affiliated to Wuhan University of Science and Technology, Wuhan, Hubei, China;

^bDepartment of Radiology, Wuhan Third Hospital, Tongren Hospital of Wuhan University, Wuhan, Hubei, China; ^cDepartment of Gastroenterology, The Third People's Hospital of Hubei Province, Wuhan, Hubei, China; ^dDepartment of Gastroenterology, Wuhan Third Hospital, Tongren Hospital of Wuhan University (Optics Valley Area), Wuhan, Hubei, China

ABSTRACT

Gastric cancer (GC) affects a large proportion of cancer patients worldwide, and the prediction of potential biomarkers can greatly improve its diagnosis and treatment. Here, miR-4268 and keratin 80 (KRT80) expression in GC tissues and cell lines was determined. The effect of downregulating miR-4268 and interfering with KRT80 expression on the viability, proliferation, apoptosis, and migration of GC cells were evaluated. The interaction between miR-4268 and KRT80 was studied using luciferase reporter and RNA pull-down assays. The western blot, CCK-8, BrdU, caspase-3 activity, Transwell assays were performed for the functional characterization. In GC tissues and cells, KRT80 expression was found to be significantly higher, while that of miR-4268 was significantly lower than the respective expressions in normal tissues and cells. Interference with KRT80 expression inhibited the viability, proliferation, and migration of GC cells and facilitated cell apoptosis *in vitro*. We further demonstrated that miR-4268 targeted KRT80 and negatively regulated its expression, and miR-4268 inhibitor alleviated the inhibitory effects of KRT80 downregulation on GC cell growth. Finally, miR-4268 may function as tumor suppressor through inhibiting PI3K/AKT/JNK pathways by targeting KRT80 in GC. Collectively, our present results indicate that the miR-4268/KRT80 axis acts as a potential therapeutic target for patients with GC.

Abbreviations: Gastric cancer (GC); MicroRNAs (miRNAs); Keratin 80 (KRT80); differentially expressed genes (DEGs); chemoradiotherapy (CRT); negative nonsense sequence (NC); radioimmunoprecipitation assay (RIPA); polyvinylidene fluoride (PVDF).

ARTICLE HISTORY

Received 7 July 2021
Revised 24 April 2022
Accepted 26 May 2022

KEYWORDS


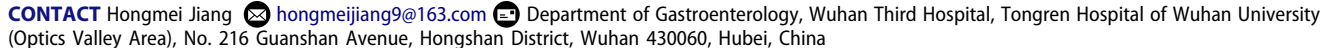
Gastric cancer; miR-4268; KRT80; proliferation; apoptosis

Introduction


Gastric cancer (GC) is the third leading cause of cancer-related deaths worldwide, with high mortality rates in many Asian countries, such as China, Japan, and South Korea [1]. Early treatment can significantly reduce the rate of mortality caused by GC [2]. Chemotherapy, radiation, and surgery are the most used treatment methods for GC [3]. However, due to high metastasis, these therapies are not sufficient to improve the survival status of patients with GC [4]. Therefore, it is important to develop alternative therapies that can resolve this issue.

Recently, numerous oncogenes and tumor suppressor genes have been demonstrated to be involved in the occurrence and development of

GC [5]. MicroRNAs (miRNAs) play a crucial role in a variety of biological processes owing to their special property of post-transcriptional regulation of gene expression [6–8]. There is growing evidence that miRNAs regulate the occurrence and development of cancer and participate in important biological functions, such as cell proliferation, migration, and invasion [9,10]. MiR-4268 has only been studied in recent years for its heterotopic expression in different tissues [11–13]. It has been shown that miR-4268 is upregulated in both aortic stenosis and radiation-resistant breast cancer cells [14,15]. Notably, a recent study has shown that miR-4268 is downregulated in GC tissues and cell lines and regulates proliferation and apoptosis

CONTACT Hongmei Jiang  hongmeijiang9@163.com 

[#]These authors contributed equally to this work.

 Supplemental data for this article can be accessed online at <https://doi.org/10.1080/15384101.2022.2085351>

© 2022 Informa UK Limited, trading as Taylor & Francis Group

in GC cells [12]. Therefore, the study of miR-4268 is of great value in developing the treatment of GC.

Keratin is an intermediate filament cytoskeleton protein, which has a special ability to maintain the structure of epithelial cells and has been identified as a representative marker of epithelial cells [16]. Previous studies have shown that keratin may serve as a molecular marker for the diagnosis of multiple types of tumors as it regulates tumor cell migration and invasion [17,18]. Keratin 80 (KRT80) has been studied as a member of keratin family found in some cancers [16,19]. For instance, it has been reported that the overexpression of KRT80 promotes breast cancer cell invasion and drug resistance [20]. Another study reported that KRT80 participates in the proliferation of colorectal cancer cells and regulates cell cycle and DNA replication pathways [16]. Recent research has shown that KRT80 overexpression promotes cell proliferation, invasion, migration, and EMT [21]. Therefore, it is also important to clarify the role of KRT80 in GC cells.

In this study, the functions of miR-4268 and KRT80 in GC were investigated, and the underlying mechanisms of miR-4268 and KRT80 were elucidated. Our results may further facilitate the validation of potential therapeutic targets for GC treatment.

Materials and methods

Bioinformatics analysis

The GSE64916 data series extracted from GEO datasets was used to screen the differentially expressed genes (DEGs) with the selection criteria of $P < 0.05$, and $\log_{2}FC > 2$. GEPIA STAD (stomach adenocarcinoma) data (<http://gepia.cancer-pku.cn/index.html>) were also used to screen the DEGs with the selection criteria of adjusted $P < 0.05$, and $\log_{2}FC > 2$. Then, the common DEGs from GSE64916 and GEPIA STAD data were uploaded to the STRING database (<https://string-db.org/>) to identify the protein-protein interaction network with a medium confidence level (0.4). Next, the prognosis of the key genes was analyzed using the Kaplan-Meier Plotter (<http://kmplot.com/analysis/>). Finally, the miRNAs combined with the key genes

were predicted using the TargetScan algorithm (v7.2, http://targetscan.org/vert_72/), and the downregulated miRNAs in GC samples were selected from the miRNA data series (GSE93415) with adjusted $P < 0.05$, and $\log_{2}FC < -1$.

Tissue collection

Forty-three pairs of cancer and para-cancerous tissue samples from patients undergoing radical gastrectomy at Puren Hospital Affiliated to Wuhan University of Science and Technology (Wuhan, China) were collected. None of the selected patients received preoperative chemoradiotherapy (CRT). The adjacent tissues were collected approximately 5 cm away from the GC. The tissue properties of the specimens were confirmed by a professional pathologist. All specimens were used in accordance with the principle of informed consent. The present study was approved by the Ethics Committee of Puren Hospital Affiliated to Wuhan University of Science and Technology (Ethics Committee number: A01401-LL201912-011). The baseline characteristics of all 43 patients with GC are presented in Table 1.

Cell culture

Human gastric epithelial cells, GES-1, and GC cell lines, including MKN74, HGC-27, AGS, and NCI-N87 were purchased from the Cell Bank of the Chinese Academy of Science (Shanghai, China). GC and gastric epithelial cells were cultured in RPMI-1640 medium (Sigma, St Louis, MO, USA) containing 10% fetal bovine serum (FBS; Gibco, New York, USA), 100 U/mL penicillin (Gibco, New York, USA), and 100 $\mu\text{g}/\text{mL}$ streptomycin (Gibco, New York, USA). All cells were cultured in 5% CO_2 at 37°C and saturated humidity and were digested with 0.25% trypsin every 2–3 days.

Cell transfection

The miR-4268 inhibitor and negative nonsense sequence (NC) were purchased from Shanghai Jima Company (Shanghai, China). The KRT80 gene-specific lentivirus packaging vector and sh-KRT80 were obtained from GuangZhou RiboBio Co., Ltd (GuangZhou, China). AGS and HGC-27

Table 1. Association between KRT80 or miR-4268 level and clinicopathologic characteristics of gastric cancer patients in the study.

Categories	N = 43	KRT80 expression		P	miR-4268 expression		P
		Low(N = 21)	High(N = 22)		Low(N = 22)	High(N = 21)	
Age (years)				0.364			0.543
< 60	24	10	14		11	13	
≥ 60	19	11	8		11	8	
Gender				0.332			0.185
Male	30	13	17		13	17	
Female	13	8	5		9	4	
Tumor size (cm)				0.215			0.760
< 5	26	15	11		14	12	
≥ 5	17	6	11		8	9	
Pathological differentiation				0.007			0.045
Moderate + well	12	10	2		3	9	
Poor	31	11	20		19	12	
Nodal status				0.022			0.003
T1 + T2	13	10	3		2	11	
T3 + T4	30	11	19		20	10	
Lymph nodes metastasis				0.002			0.014
Negative	18	14	4		5	13	
Positive	25	7	18		17	8	
TNM stage				0.029			0.002
I	8	7	1		1	7	
II	9	5	4		2	7	
III	26	9	17		19	7	
CEA (ng/ml)				0.009			0.009
≤ 5	36	21	15		15	21	
> 5	7	0	7		7	0	
CA199 (U/ml)				0.009			0.001
≤ 35	9	8	1		0	9	
> 35	34	13	21		22	12	
Histopathological diagnosis				0.619			0.365
Tubular	32	16	16		16	16	
Hybrid	1	0	1		0	1	
Mucinous	4	1	3		2	2	
Signet ring cell	3	2	1		1	2	
Others ^a	3	2	1		3	0	
<i>H.pylori</i>				0.262			0.312
Positive	22	12	10		9	13	
Negative	21	9	12		13	8	
MMR status				0.005			0.007
Deficient	25	20	5		6	19	
Intact	18	1	17		16	2	

^aothers: papillary adenocarcinoma, 1 case; squamous cell carcinoma, 1 case; undifferentiated carcinoma, 1 case. CEA: carcinoembryonic antigen. CA199: carbohydrate antigen 199. MMR: mismatch repair.

cells were cultured for 24 h, and LipofectamineTM 2000 (Invitrogen, Carlsbad, CA, USA) was used to induce transfection of 50 nM miR-4268 inhibitor, 50 nM sh-KRT80, and 50 nM NC, respectively. After oscillating and blending, polybrene was placed at room temperature for 30 min. Then, the mixture was incubated for 30 min at 25°C, and the polybrene infection enhancer was added and cultured for 24–48 h. RNA was extracted from the cells and the target gene expression was assessed using qRT-PCR.

qRT-PCR

AGS and HGC-27 cells were harvested at the logarithmic growth phase, and miRNAs and total RNA were extracted using the miRNeasy EFPE kit (BioTeke, Beijing, China) and Trizol kit (Invitrogen, CA, USA), respectively, according to the manufacturer instructions. The absorbance value (A) of RNA was determined using the photometer method, and the ratio of A260/A280 for RNA samples was determined to be within

Table 2. Primer sequences.

Genes	Primer sequences
KRT80	Forward:5'-GGCCCTCAATGATAAATTTGC-3' Reverse:5'-CGGCCCTGATATTCCTCATA-3'
GAPDH	Forward:5'-GTCAACGGATTGGTCGTAT-3' Reverse:5'-TGGTGATGGGATTTCCATTG-3'
U6	Forward:5'-CAGCACATATACTAAAATTGGAACG-3' Reverse:5'-ACGAATTTGCCTGCATCC-3'

1.8 ~ 2.1, and the extracted RNA was qualified and used in the following reaction. A portion of each sample (50 μ L out of 300 μ L) was subjected to cDNA synthesis. The Mir-X miRNA First Strand synthesis kit (TaKaRa-Bio, Shiga, Japan) was used for the reverse transcription of miRNAs to synthesize the first-strand cDNA. Using U6 as an internal reference, the TaqMan[®] microRNA assay kit (Thermo Fisher Scientific, Waltham, MA, USA) was used to conduct the qRT-PCR analysis of miR-4268.

For mRNA quantification, 1 μ g RNAs were reverse-transcribed to cDNA using the One Step PrimeScript cDNA synthesis Kit (Thermo Fisher Scientific, Waltham, MA, USA), and qRT-PCR was performed using SYBR Green PCR Master Mix (Thermo Fisher Scientific, Waltham, MA, USA), with GAPDH as the internal reference. PCR reactions were carried out in a volume of 20 μ L containing 50 ng DNA template on ABI 7500 platform. The parameters were set as follows: 95°C for 5 min, 95°C for 5s, 60°C for 30s, 72°C for 45s, 36 cycles, 60°C for 5 min, and the collection of data. The data were analyzed using the method of $2^{-\Delta\Delta C_t}$. Primer sequences are listed in Table 2.

Western blot analysis

After transfection for 48 h, AGS and HGC-27 cells were subjected to protein extraction using the radioimmunoprecipitation assay (RIPA) buffer (Cell Signaling Technology, Danvers, MA, USA), and the protein concentration was determined using the standard BCA protein assay kit (Pierce, Rockford, IL, USA). After separating 30 μ g of protein using a 10% SDS-PAGE, the protein was transferred to the polyvinylidene fluoride (PVDF) membrane using semi-dry membrane transfer method after cutting out membranes based on the different molecular weight of proteins. After

blocking nonspecific binding sites using 5% skimmed milk for 60 min. These membranes were incubated with primary antibodies including anti-KRT80 (1:800, cat. no. 16,835-1-AP, ProteinTech Group, IL, USA), anti-PI3K (1:1000, cat. no. 4257 Cell Signaling Technology, Danvers, MA, USA, USA), anti-p-PI3K (1:500, cat. no. 17,366, Cell Signaling Technology, USA), anti-AKT (1:1000, cat. no. 2902, Cell Signaling Technology, USA), anti-p-AKT (1:300, cat. no. 9614, Cell Signaling Technology, USA), anti-JNK (1:1,000, cat. no. ab124956, Abcam, Cambridge, MA, USA), anti-p-JNK (1:1,000, cat. no. ab47337, Abcam) and anti-GAPDH (1:1000, ab181602, Abcam) overnight at 4°C, and then blocked with 5% skimmed milk TBST for 2 h at 25°C. These PVDF membranes were incubated with the corresponding secondary antibody (1:5,000, Cell Signaling Technology) at 37°C for 30 min. After washing with PBST, these membranes were treated with enhanced chemiluminescence (ECL) reagent (Little Chalfont, Buckinghamshire, UK). The membrane was then exposed in a darkroom for further development and fixation.

CCK-8 assay

CCK-8 proliferation assay kit (Beyotime, Shanghai, China) was performed to evaluate the cell viability. Cells were collected during the logarithmic growth phase, digested with trypsin, and inoculated into a 96-well plate at a concentration of 5000 cells per well. The cells were cultured for 0, 24, 48, and 72 h. The culture medium was removed from each well and replaced with 100 μ L RPMI-1640 medium and 10 μ L CCK-8 reagent per well, and the absorbance at 450 nm was measured using a microplate reader (Bio-Rad Laboratories, Hercules, CA, USA). Then, the cell proliferation curve was obtained after 2 h of culturing at 37°C in the dark.

BrdU assay

Cells were seeded at a density of 1×10^4 cells per well into 96-well plates, and BrdU reagent (CPK0010; BrdU Cell Proliferation Assay Kit; Frdbio, Wuhan, China) was added at a cell density of approximately 60%. After 48 h of culture, the

supernatant was discarded, and 100 μ L of cell fixative was added to each well and fixed for 30 min at 25°C. After adding 100 μ L of cell denaturation solution into each well, the cells were denatured for 10 min at 25°C. Then, 100 μ L BrdU reagent was added to each well, and after adding diluted anti-BrdU antibody (1:1,000; cat. no. ab8152; Abcam), the plate was vortexed slightly at 37°C for 1 h. Subsequently, 100 μ L of goat anti-mouse IgG Alexa Fluor® 647-conjugated secondary antibody (1:500; cat. no. ab150115; Abcam) was added and the plate was incubated for 1 h at 37°C. Then, 100 μ L of TMB substrate solution was added and the reaction was conducted at 25°C for 10 min. Finally, 100 μ L of substrate termination fluid was added, and OD450 were measured.

Caspase-3 activity assay

The activity of caspase-3 in AGS and HGC-27 cells was measured using the caspase-3 activity assay kit (Jining Shiye, Shanghai, China). AGS and HGC-27 cells (2×10^6) were centrifuged at 4°C for 3 min at $500 \times g$ to harvest the cells. After washing with cold PBS, 100 μ L cold cracking buffer was added to the cells, and oscillated for 15s using a high-speed vortex. The cells were then incubated on ice for 15 min, with oscillation every 5 min for 15s. After centrifugation, the lysed supernatant containing 30 μ g of protein was added to 90 μ L buffer and 10 μ L Ac-LEHD-pNA, and then incubated in the dark at 37°C for 1–2 h. Relative caspase-3 activity was evaluated based on the ratio of the light absorption value of apoptosis-induced cells to that of the control cells.

Transwell assay

AGS and HGC-27 cells were cultured in basal medium for 6–8 h to remove the serum. The digested cells were then resuspended in basal medium, and the cell count was adjusted to 5×10^5 /mL. About 200 μ L of cell suspension was added into the Transwell chamber, and then, 500 μ L of medium containing 5% FBS was added to the lower chamber, and the plate was incubated for 24 h. After culture, the cells on the bottom surface

of the upper chamber were carefully wiped off with a wet cotton swab and stained with 1% crystal violet (Sigma, St Louis, MO, USA) for 30 min. A light microscope (Olympus, Tokyo, Japan) was used to count five random fields, and the average value was recorded.

Luciferase reporter assay

The putative sequences of the miR-4268 binding site in KRT80 3'UTR was cloned into the pmirGLO luciferase expression vector (Promega, Madison, WI, USA). The KRT80 mutated sequences with two binding sites (position 295–302 as KRT80-MUT1 and position 922–928 as KRT80-MUT2) of miR-6248 were obtained using the Quik-Change™ Site-Directed Mutagenesis Kit (Stratagene, CA, USA). KRT80 wild-type and mutant reporter vectors were co-transfected with miR-4268 mimic and miR-NC into HGC-27 and AGS cells. Luciferase activity was assessed using the Glomax 20/20 Luminometer (Promega, Madison, WI, USA) at 48 h post transfection.

RNA pull-down assay

RNA pull-down was performed using the Magnetic RNA pull-down kit (Pierce, Rockford, IL, USA) according to the manufacturer's instructions. In brief, total RNA was extracted from HGC-27 and AGS cells. About 200 pmol of biotin-labeled miR-4268 mimic and miR-4268-NC were mixed with 500 μ g of magnetic beads. Then, 100 μ g of total RNA was added to form an RNA-RNA complex, which could bind to streptavidin-labeled magnetic beads, and thus, be separated from other components in the incubation solution. RNA bound to the magnetic beads was eluted and then detected using qRT-PCR.

Statistical analysis

SPSS (IBM SPSS 22.0, Chicago, IL, USA) was used for the data analysis, and the data results are presented as mean \pm SD. All data were normally distributed as determined by Kolmogorov-Smirnov tests. Comparison between the two groups was performed using the unpaired student's t-test.

One-way ANOVA followed by Dunnett's or Tukey's post hoc tests were performed to determine the differences among the experimental groups. Correlation analysis between miR-4268 and KRT80 expression in GC tissues was performed using Pearson's correlation coefficient. The effect of KRT80 and miR-4268 on clinicopathologic characteristics was analyzed using Fisher exact test. Statistical significance was set at $P < 0.05$.

Results

KRT80 and miR-4268 are potentially significant participants in GC

First, we intersected the DEGs of GSE64916 and GEPIA STAD (stomach adenocarcinoma) data. A total of 17 common DEGs were identified (Figure 1(a)). To further identify one significant gene among the 17 genes, we uploaded them to the STRING database and found that KRT8, KRT18,

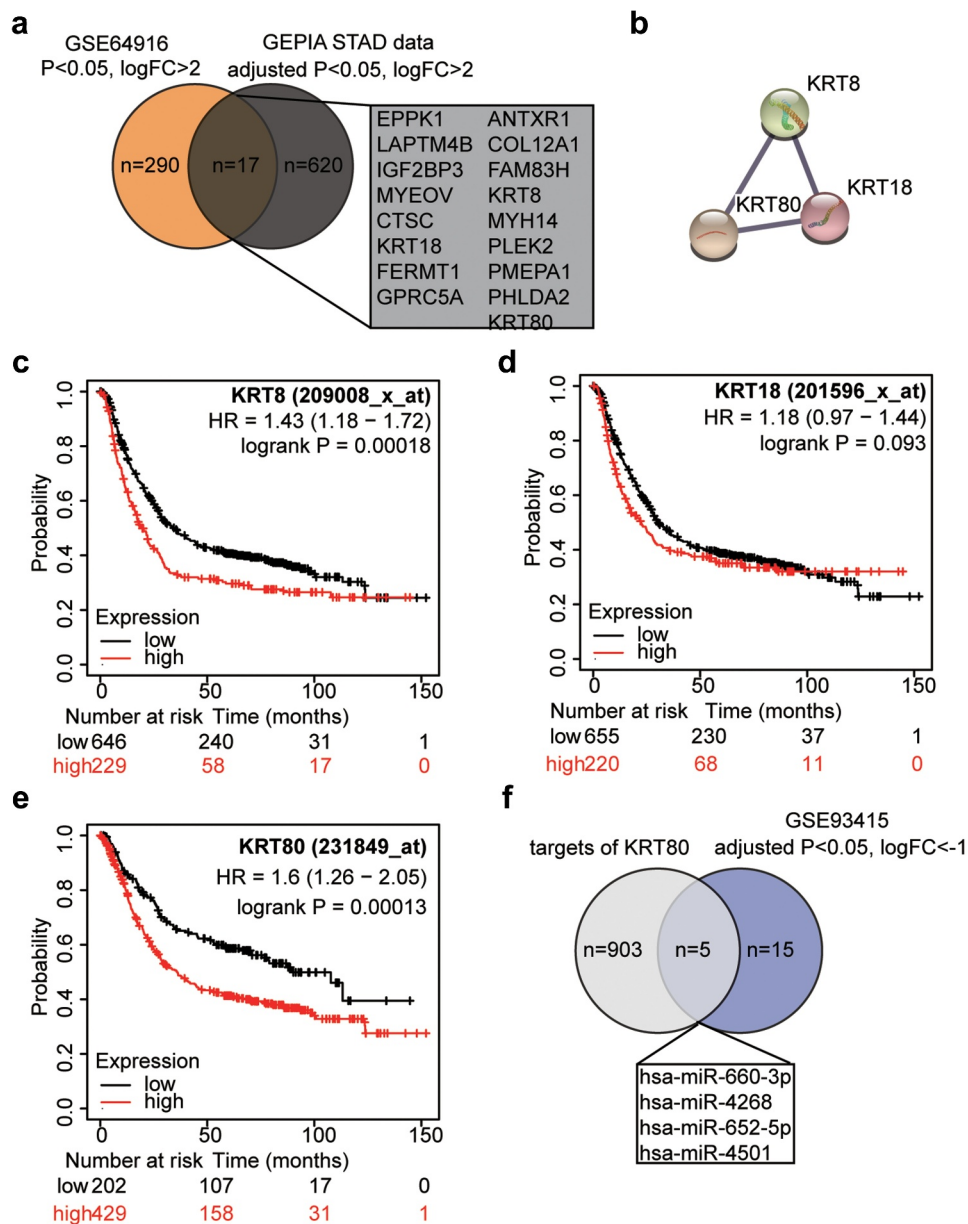


Figure 1. KRT80 and miR-4268 can be potentially significant participants in GC. (a) A Venn diagram showing the intersection between the list of DEGs of GSE64916 data series and the DEGs of GEPIA STAD (stomach adenocarcinoma) data. FC: fold change. (b) The STRING analysis of the 17 genes from Figure A. (c-e) The overall survival outcomes of KRT8, KRT18 and KRT80 in GC calculated using km plotter (<http://kmplot.com/analysis/>). (f) A Venn diagram showing that there were five miRNAs that were the candidate targets of KRT80 and also the significantly downregulated miRNAs in GC in GSE93415 data series.

and KRT80 were associated with each other (Figure 1(b)). All three genes have been reported to exhibit cancer genesis -related functions in GC [21–23]. We then obtained the prognosis results for these three genes. KRT8 and KRT80 could distinguish between good and poor survival outcomes in GC patients (Figure 1(c, e)), whereas KRT18 could not (Figure 1(d)). KRT80 showed the most significance; thus, it was selected as the gene of interest. Thereafter, we predicted the miRNAs combined with KRT80 using the TargetScan algorithm. Through intersecting the predicted miRNAs and the differentially expressed miRNAs in the GSE93415 data series, we identified five common miRNAs in the two datasets, including miR-660-3p, miR-4268, miR-652-5p, and miR-4501 (figure 1f). miR-4268 has been reported as a suppressor of GC [12]. Therefore, this has been very limitedly studied.

KRT80 is highly expressed in GC and promotes the proliferation and migration of GC cells *in vitro*

We tested the mRNA and protein expression of KRT80 in GC and adjacent normal tissues, and found that KRT80 mRNA and protein expression in GC tissues were significantly increased by approximately 3.5- and 1.5 times, respectively, compared to that in normal tissue ($P < 0.0001$ and $P = 0.0002$; Figure 2(a, b)). The relationship between KRT80 expression and the clinicopathological features was then analyzed. KRT80 expression was not associated with age, sex, tumor size, histopathological diagnosis and *H.pylori* infection; however, it was closely associated with lymph node metastasis, nodal status, CEA, CA199, pathological differentiation, TNM stage and defective mismatch repair (Table 1). Next, we assessed KRT80 expression in GC cell lines and normal gastric epithelial cells. Consistent with the clinical results, the expression level of KRT80 in GC cell lines was also higher than that in GES-1 cells ($P < 0.001$; Figure 2(c)). To study the effect of KRT80 on the biological function of GC cells *in vitro*, we first designed a KRT80 gene-specific lentivirus packaging vector, sh-KRT80. qRT-PCR analysis results showed that sh-KRT80 successfully inhibited KRT80 expression in AGS and HGC-27 cells and

reduced the expression of KRT80 mRNA by approximately 70% ($P < 0.001$; Figure 2(d)). Western blot analysis also showed a successful reduction in KRT80 protein levels ($P < 0.001$; Figure 2(e)). To further evaluate the effect of KRT80, we found that the viability of GC cells cultured for 48 and 72 h decreased after silencing KRT80, and it further decreased significantly over time ($P < 0.001$; figure 2(f)). Additionally, we clarified that the proliferation of HGC-27 and AGS cells transfected with sh-KRT80 decreased to half compared to that of NC group using the BrdU assay ($P < 0.001$; Figure 2(g)). Next, we analyzed the activity of caspase-3 to evaluate the effect of KRT80 on GC cell apoptosis. The results showed that the activity of caspase-3 increased approximately 1.7 times after silencing KRT80 ($P < 0.001$; Figure 2(h)). Transwell assay results revealed the knockdown of KRT80 reduced the migration of GC cells (Figure 2(i)). These results confirmed that KRT80 has a certain influence on the function of GC cells, and that the upregulation of KRT80 promoted the viability, proliferation, and migration of HGC-27 and AGS cells *in vitro*, and inhibited cell apoptosis.

KRT80 is a potential target gene of miR-4268

To investigate the mechanism of KRT80 in GC cells, we screened its upstream miRNA, miR-4268. TargetScan search revealed that miR-4268 and KRT80 possess two binding sites (Figure 3(a)). A luciferase reporter assay was performed to determine whether miR-4268 directly affects KRT80 genes in AGS and HGC-27 cells. In cells co-transfected with the miR-4268 mimic, the luciferase activity of wild-type KRT80 3'UTR with the miR-4268 binding site decreased by 50%, and the luciferase activity decreased by 30% when only a single binding site of KRT80 3'UTR was mutated, while the luciferase activity of the builder with mutated binding sites was not significantly changed ($P < 0.001$; Figure 3(b)). The RNA pull-down assay results revealed that the binding of biotin-labeled miR-4268 to KRT80 increased ($P < 0.001$; Figure 3(c)). Additionally, we assessed the level of miR-4268 in the clinical tissues and found that the level of miR-4268 in cancer tissue decreased by approximately 70% compared to that in normal

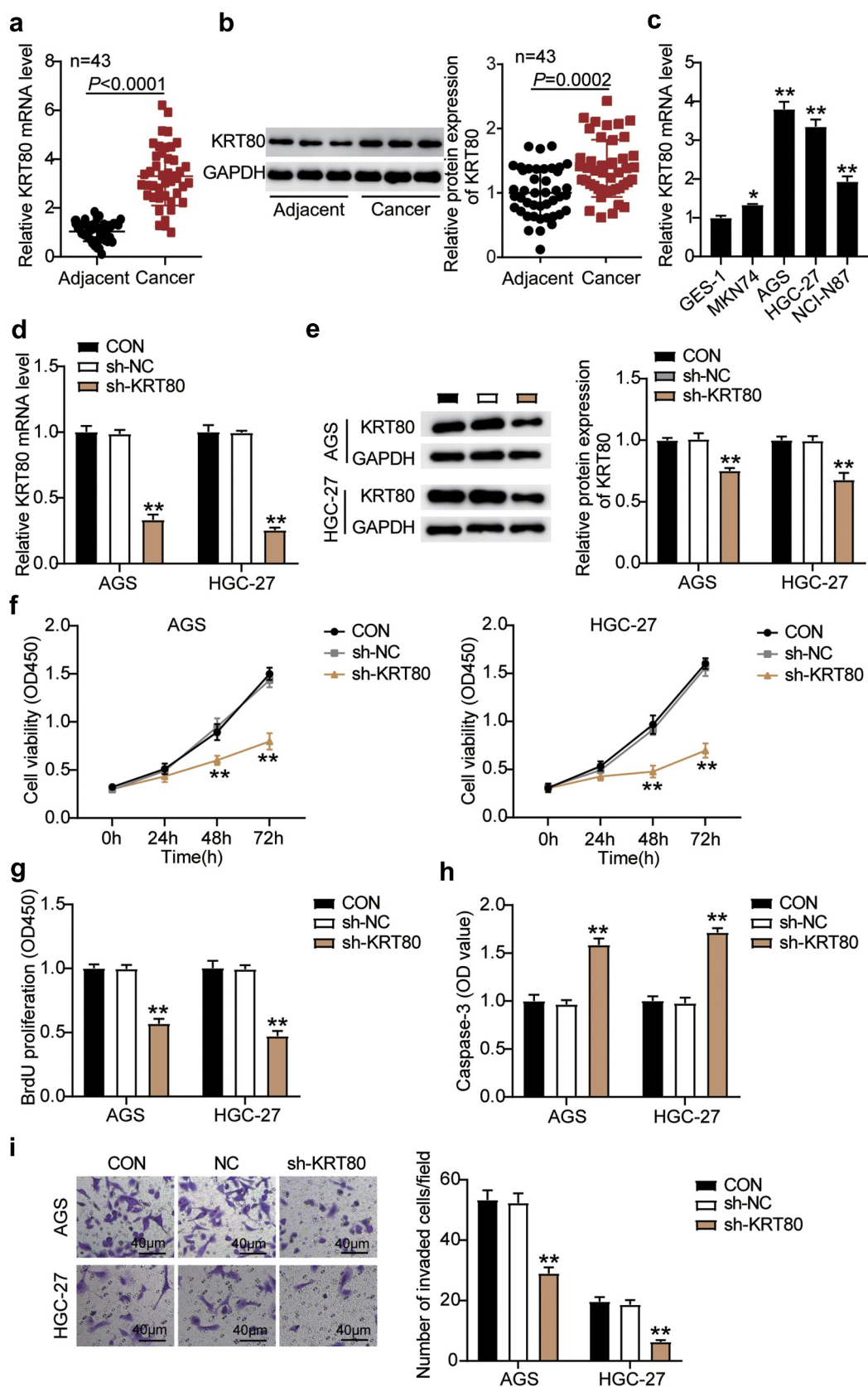


Figure 2. KRT80 is highly expressed in GC and promotes the proliferation and migration of GC cells *in vitro*. (a) Real-time PCR analysis of KRT80 mRNA expression in GC tissues and adjacent normal tissues. (b) Western blotting analysis of KRT80 protein expression in GC tissues and adjacent normal tissues. (c) KRT80 mRNA levels in GES-1, MKN74, AGS, HGC-27 and NCI-N87 cells were examined using real-time PCR. * $P < 0.05$, ** $P < 0.001$ vs. GES-1. (d) Real-time PCR analysis of the mRNA expression of KRT80 in AGS

tissue ($P < 0.0001$; Figure 3(d)). Furthermore, the relationship between miR-4268 expression and the clinicopathological features was assessed and we found that miR-4268 expression was associated with lymph node metastasis, nodal status, CEA, CA199, pathological differentiation, and TNM stage, but not with age, sex, tumor size, and histopathological diagnosis (Table 1). Pearson analysis results revealed a negative correlation between miR-4268 and KRT80 in GC ($P < 0.0001$; Figure 3(e)). Moreover, at the cellular level, miR-4268 expression in GC cells was found to be lower than that in GES-1 cells ($P < 0.001$; figure 3(f)).

Effects of miR-4268/KRT80 axis on GC cells

To further investigate whether miR-4268 plays a specific role through targeting KRT80 in GC cells, miR-4268 was downregulated by miR-4268 inhibitor in AGS and HGC-27 cells. RT-PCR analysis results showed that after transfection with the miR-4268 inhibitor, the expression miR-4268 was reduced by approximately 70% and that of KRT80 increased by approximately 3.5-fold ($P < 0.001$; Figure 4(a), Supplementary Figure 1A). Moreover, the expression level of KRT80 upregulated through the addition of miR-4268 inhibitor was decreased by sh-KRT80 ($P < 0.001$; Figure 4(a) and Supplementary Figure 1B). Western blot analysis results indicated that KRT80 protein expression was in consensus with that of qRT-PCR ($P < 0.001$; Figure 4(b) and Supplementary Figure 1C). Next, we investigated the biological functions of GS cells. The results of CCK-8 assay revealed that the cell viability of AGS and HGC-27 cells after transfection with miR-4268 inhibitor was 1.3 times higher than that of the NC group, and the viability reduced significantly upon sh-KRT80 transfection ($P < 0.001$; Figure 4(c)). Furthermore, the level of cell proliferation was assessed, and it was found that the cell proliferation ability of

cells increased after interference with miR-4268, and furthermore, sh-KRT80 suppressed the effect of miR-4268 inhibitor ($P < 0.001$; Figure 4(d)). Additionally, the silencing miR-4268 reduced caspase-3 activity, while caspase-3 activity was increased in the sh-KRT80 group compared to that in the sh+inhibitor group ($P < 0.001$; Figure 4(e)). In the Transwell assay, we found that the downregulation of miR-4268 reduced the migration of GC cells and reversed the decline caused by KRT80 knockdown ($P < 0.001$; figure 4(f)).

MiR-4268 inhibited PI3K/AKT/JNK pathways by downregulating KRT80

Finally, we examined the effect of miR-4268 on PI3K/AKT/JNK pathways by regulating KRT80. As shown in Figure 5, compared with inhibitor-NC group, miR-4268 inhibitor transfection significantly upregulated the expressions of p-PI3K, p-AKT and p-JNK ($P < 0.001$). Meanwhile, compared with sh-NC group, KRT80 knockdown showed the opposite trend, the expressions of p-PI3K, p-AKT and p-JNK were increased significantly ($P < 0.001$). Additionally, KRT80 knockdown partially reversed the promoting effect of miR-4268 inhibitor on the phosphorylation of PI3K/AKT/JNK pathways.

Discussion

RNA regulation is of great value in cancer therapy and may be transformed into a novel technology with significant therapeutic applications [24]. KRT80 has been identified as a biomarker for poor prognosis of various tumors, including breast cancer and colorectal cancer [16,20]. In GC, it was revealed in only one study that the ectopic expression of KRT80 can promote cell proliferation, invasion, migration, and EMT, and that its effect could be regulated by the circPIP5K1A/miR-671-5p axis [21]. Consistent with a previous study, we

and HGC-27 cells treated with sh-KRT80 and sh-NC. (e) The expression of KRT80 in both AGS and HGC-27 cells was examined using western blotting after transfection with sh-KRT80 and sh-NC. (f) The effect of KRT80 silencing on the growth rate of both AGS and HGC-27 cells examined using the CCK-8 assay. (g) The effect of KRT80 silencing on proliferation in both AGS and HGC-27 cells examined using the BrdU assay. (h) The effect of KRT80 silencing on caspase-3 activity in both AGS and HGC-27 cells examined using the caspase-3 activity assay. (i) The effect of KRT80 silencing on the migration of both AGS and HGC-27 cells examined using a Transwell assay. ** $P < 0.001$ vs. Con. Con, blank control.

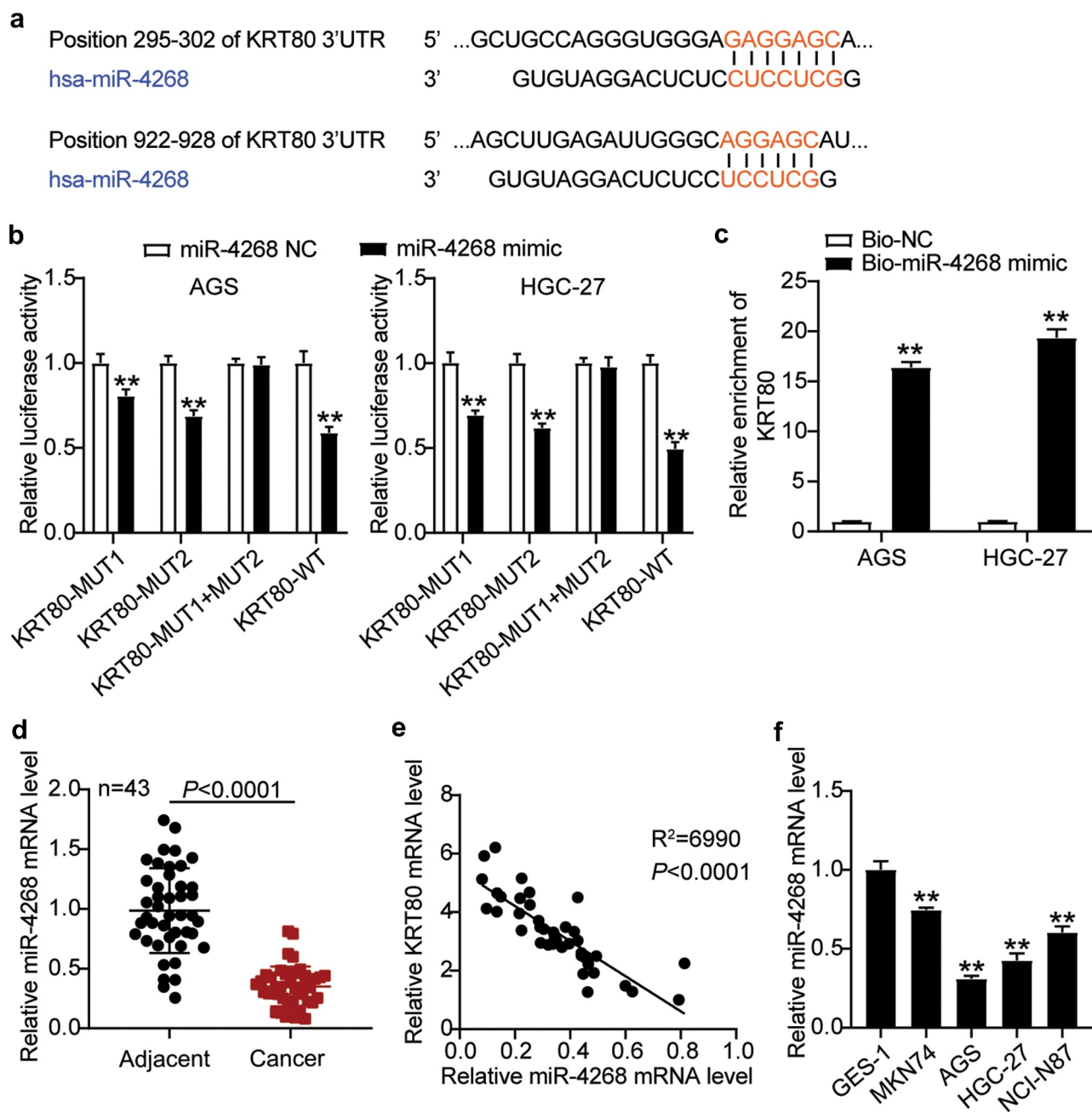


Figure 3. KRT80 is a potential target gene for miR-4268. (a) Predicted miR-4268 binding sites in the 3'UTR of wild-type (KRT80-WT) and mutant (KRT80-MUT1, KRT80-MUT2 and KRT80-MUT1+ MUT2) KRT80 sequences. (b) Luciferase reporter assays were performed 48 h after co-transfection of AGS and HGC-27 cells with miR-4268-NC or miR-4268 mimic and a luciferase vector encoding the wild-type or mutant KRT80 3'UTR region. $**P < 0.001$ vs. miR-4268 NC. (c) Enrichment of KRT80 in magnetic bead eluent of miR-4268-NC or miR-4268 mimic measured by RNA pull-down assay. $**P < 0.001$ vs. Bio-NC. (d) Real-time PCR analysis of miR-4268 expression in GC tissues and adjacent normal tissues. (e) The correlation between miR-4268 and KRT80 in GC tissues determined by Pearson analysis. (f) miR-4268 levels in GES-1, MKN74, AGS, HGC-27 and NCI-N87 cells were examined using real-time PCR. $**P < 0.001$ vs. GES-1.

found a basal increase in KRT80 expression in GC tissues, and silencing KRT80 can restrain the viability, proliferation, and migration of GC cells and promote apoptosis. In addition, our bioinformatics

analysis and cell functional experiments showed that miR-4268 was upstream of KRT80, thereby reversing the positive effect of KRT80 on GC cells. These results suggest that KRT80 might play a

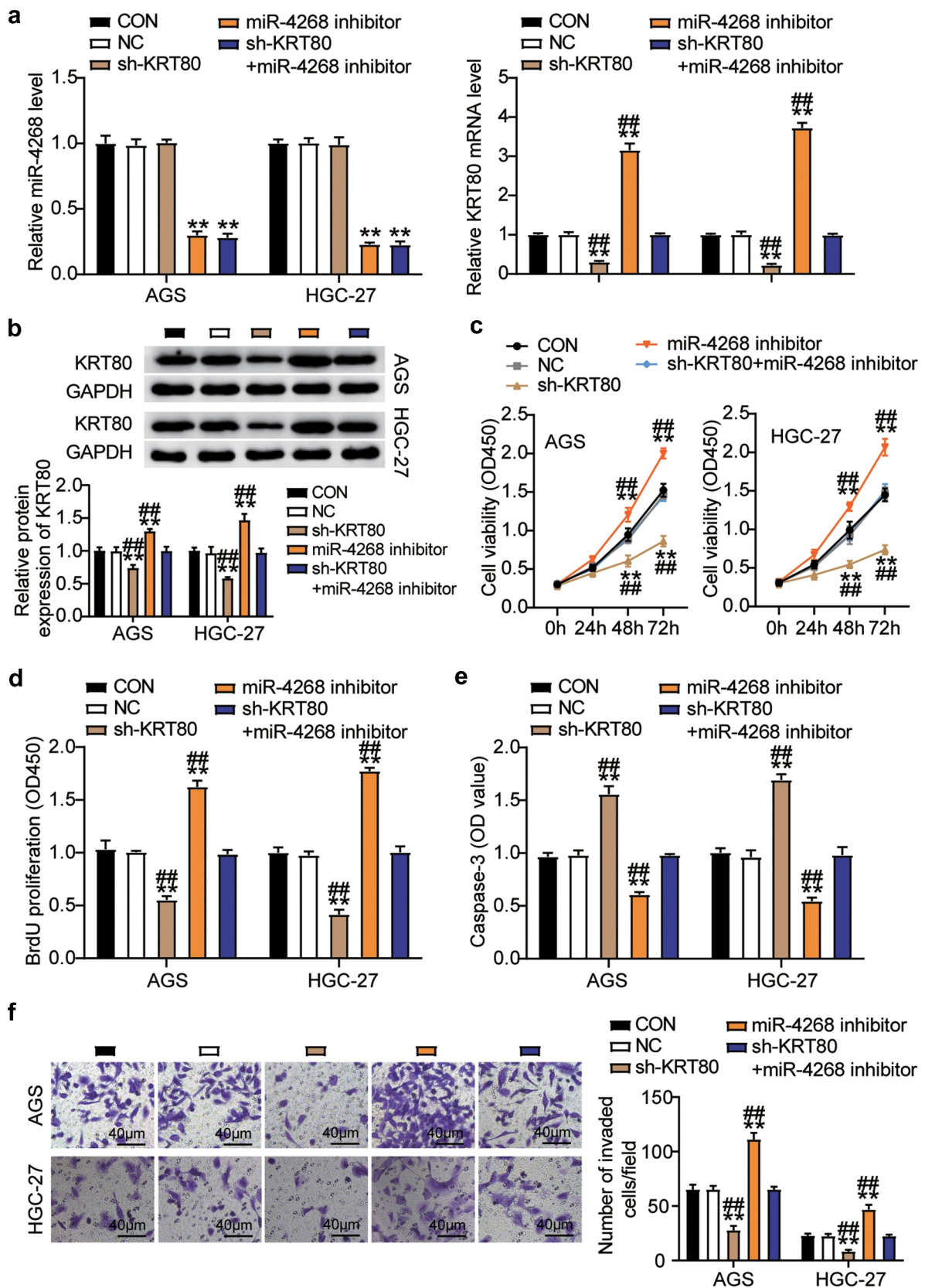


Figure 4. The effects of the miR-4268/KRT80 axis on GC cells. (a) Real-time PCR analysis of the expression of miR-4268 and KRT80 mRNA in AGS and HGC-27 cells treated with sh-KRT80 or miR-4268 inhibitor. (b) The expression of KRT80 in both AGS and HGC-27 cells was examined using western blotting after transfection with sh-KRT80 or miR-4268 inhibitor. (c) The effect of KRT80 or miR-4268 silencing on the growth rate of both AGS and HGC-27 cells examined using the CCK-8 assay. (d) The effect of KRT80 or miR-

crucial role in regulating the function of GC cells *in vitro* via multiple regulators.

Recent studies have shown that abnormal expression of miRNAs in tissues contributes to the occurrence of GC, and miRNAs can be used as predictive biomarkers for the diagnosis of GC [5,25,26]. For example, MiR-142-5p has been found to contribute to GC progression through regulating the expression of ULK1 [27]. MiR-20a-5p acts as a cancer promoter in GC through regulating the expression of WTX gene [28]. Based on this phenomenon, we determined the upstream miRNA, miR-4268, that can target and regulate KRT80 in GC using bioinformatics analysis. After reviewing the literature, we found only one study wherein it was shown that miR-4268 inhibited cell proliferation and cell cycle, as well as induced cell apoptosis in GC through targeting Rab6B [12]. Similar to this above previous study, we found that miR-4268 knockdown promoted the viability, proliferation, and migration of GC cells and inhibited apoptosis, suggesting the inhibitory effect of miR-4268 on GC cells. However, we also found that miR-4268 binds to the 3'UTR of KRT80 and negatively regulate its expression level in GC tissues and cells. We further attempted to elucidate the direct biological function of the miR-4268/KRT80 axis in GC. The effect of miR-4268 inhibitor on AGS and HGC-27 cells was in contrast to that of silencing KRT80, which promoted the activity, proliferation, and migration of GC cells and inhibited apoptosis. Moreover, the addition of miR-4268 inhibitor reduced the effect of sh-KRT80 on GC cell function. These results revealed that the miR-4268/KRT80 axis plays an important role in the growth of GC cells.

To further investigate miR-4268/KRT80 axis-mediated signaling pathway in GC, one known signaling pathway were explored. One previous report has demonstrated that miR-4268 impairs GC cell survival via inhibiting AKT/JNK signaling pathways [12], and KRT80 involves in the regulation of GC cell proliferation via activating PI3K/AKT pathway [21].

Potentially, the AKT/JNK and PI3K/AKT pathways may be involved in the regulation of miR-4268/KRT80 axis in the occurrence and development of GC. In this study, we found that transfection of miR-4268 inhibitor upregulated the phosphorylation levels of PI3K/AKT/JNK pathway-related proteins, which were downregulated in GC cells transfected with sh-KRT80. These findings suggest that miR-4268 may mediate GC development through inhibiting PI3K/AKT/JNK pathways by directly targeting KRT80.

MiRNAs are known to play an important role in regulating the cancer markers, such as invasion, metastasis, proliferation, resting death, apoptosis, and genomic instability, and have gradually become the biomarkers for the diagnosis, prognosis, and prognosis of cancer treatment [29]. In this study, however, we were limited in terms of the clinical sample acquisition cycle and were unable to investigate the association between miR-4268 and GC patient outcomes. Secondly, the function of miR-4268 *in vivo* is yet to be validated. Finally, the upstream gene regulators of miR-4268 in GC still require to be studied.

In conclusion, we found that miR-4268 was downregulated, and KRT80 was upregulated in GC. Additionally, miR-4268 negatively regulates the expression of its downstream target gene, KRT80. And miR-4268 may serves as a tumor suppressor on GC progression through regulating PI3K/AKT/JNK signaling pathways via inhibiting KRT80 expression. These results revealed that the miR-4268/KRT80 axis is involved in the growth of GC cells. Our findings highlight the potential of these molecules as therapeutic targets in GC diagnosis and treatment.

Authors' contributions

FZ, GXW and HMJ performed the experiments and data analysis. FZ, GXW and WJY conceived and designed the study. All authors read and approved the manuscript.

4268 silencing on proliferation in both AGS and HGC-27 cells examined using the BrdU assay. (e) The effect of KRT80 or miR-4268 silencing on caspase-3 activity in both AGS and HGC-27 cells examined using the caspase-3 activity assay. (f) The effect of KRT80 or miR-4268 silencing on the migration of both AGS and HGC-27 cells examined using a Transwell assay. **P < 0.001 vs. Con; ###P < 0.001 vs. sh-KRT80+ miR-4268 inhibitor. Con, blank control.

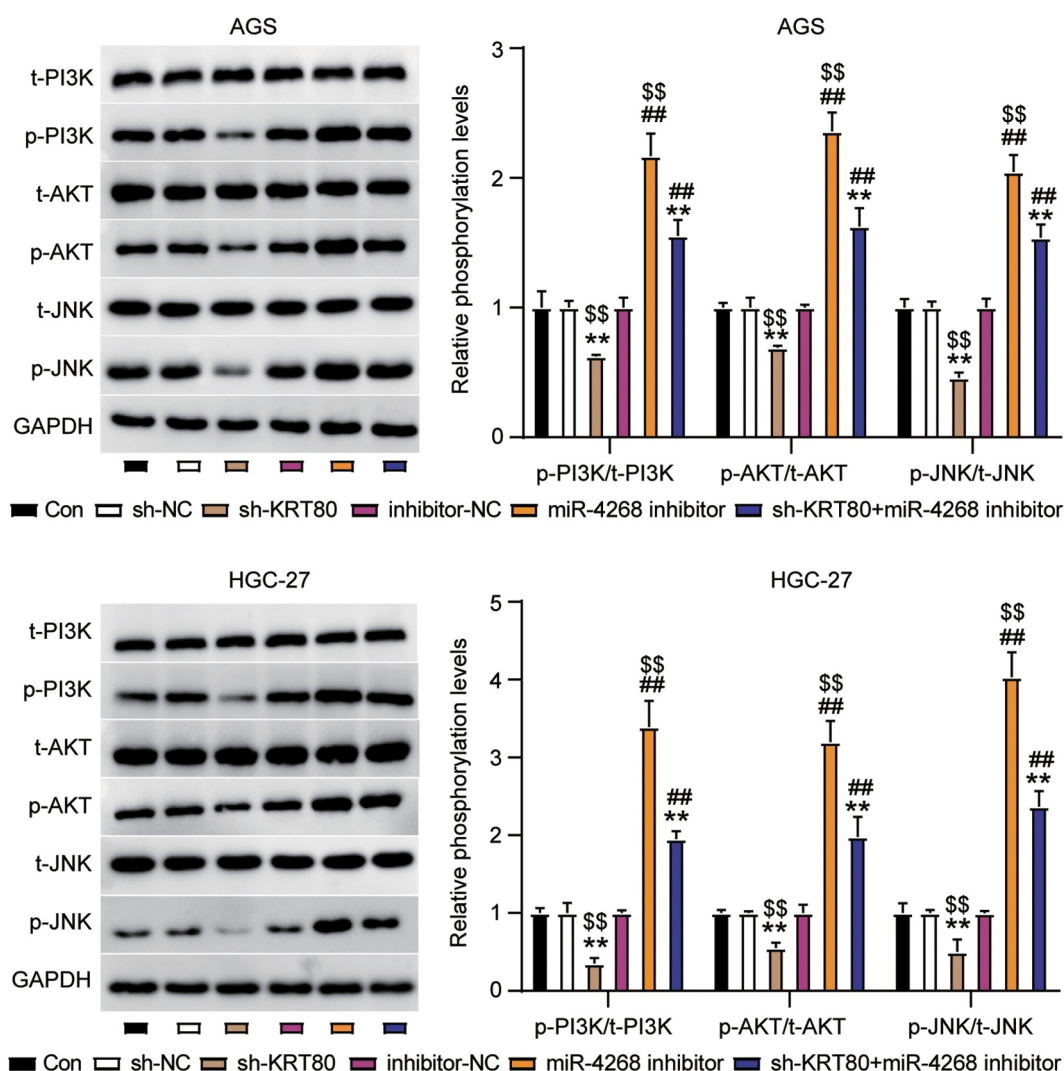


Figure 5. MiR-4268 inhibited PI3K/AKT/JNK pathways by downregulating KRT80. The phosphorylation of PI3K/AKT/JNK pathways in AGS and HGC-27 cells transfected with sh-NC, sh-KRT80, inhibitor-NC, miR-4268 inhibitor and sh-KRT80+ miR-4268 inhibitor were evaluated by western blotting. ** $P < 0.001$ vs. sh-NC; ## $P < 0.001$ vs. inhibitor-NC; \$\$\$ $P < 0.001$ vs. sh-KRT80+ miR-4268 inhibitor. Con, blank control.

Disclosure statement

No potential conflict of interest was reported by the author(s).

Funding

Funding information is not available.

Consent to publish

Consent for publication was obtained from the participants.

Data availability

The datasets used and/or analyzed during the current study are available from the corresponding author on reasonable request.

Ethical approval

The present study was approved by the Ethics Committee of Puren Hospital Affiliated to Wuhan University of Science and Technology (reference number A01401-LL201912-011). The processing of clinical tissue samples is in strict compliance with the ethical standards of the Declaration of Helsinki.

Informed consent from participants

All patients signed written informed consent.

References

- [1] Rawla P, Barsouk A. Epidemiology of gastric cancer: global trends, risk factors and prevention. *Prz Gastroenterol.* **2019**;14(1):26–38.
- [2] Kwon HN, Lee H, Park JW, et al. Screening for early gastric cancer using a noninvasive urine metabolomics approach. *Cancers (Basel).* **2020**;12(10):2904.
- [3] Fitzmaurice C, Allen C, Barber RM, et al. Global, regional, and national cancer incidence, mortality, years of life lost, years lived with disability, and disability-adjusted life-years for 32 cancer groups, 1990 to 2015: a systematic analysis for the global burden of disease study. *JAMA Oncol.* **2017**;3(4):524–548.
- [4] Chen Z, Gao Y, Gao S, et al. MiR-135b-5p promotes viability, proliferation, migration and invasion of gastric cancer cells by targeting krüppel-like factor 4 (KLF4). *Arch Med Sci.* **2020**;16(1):167–176.
- [5] Cao C, Sun D, Zhang L, et al. miR-186 affects the proliferation, invasion and migration of human gastric cancer by inhibition of twist1. *Oncotarget.* **2016**;7(48):79956–79963.
- [6] Fernández-Hernando C, Suárez Y, Rayner KJ, et al. MicroRNAs in lipid metabolism. *Curr Opin Lipidol.* **2011**;22(2):86–92.
- [7] Najafi-Shoushtari SH. MicroRNAs in cardiometabolic disease. *Curr Atheroscler Rep.* **2011**;13(3):202–207.
- [8] Lee YS, Dutta A. MicroRNAs in cancer. *Annu Rev Pathol.* **2009**;4(1):199–227.
- [9] Li H, Yao G, Zhai J, et al. LncRNA FTX promotes proliferation and invasion of gastric cancer via miR-144/ZFX axis. *Onco Targets Ther.* **2019**;12:11701–11713.
- [10] Cao Y, Xiong JB, Zhang GY, et al. Long noncoding RNA UCA1 regulates PRL-3 expression by sponging MicroRNA-495 to promote the progression of gastric cancer. *Mol Ther Nucleic Acids.* **2020**;19:853–864.
- [11] Wang S, Yuan Q, Zhao W, et al. Circular RNA RBM33 contributes to extracellular matrix degradation via miR-4268/EPHB2 axis in abdominal aortic aneurysm. *PeerJ.* **2021**;9:e12232.
- [12] Zhao L, Xue M, Zhang L, et al. MicroRNA-4268 inhibits cell proliferation via AKT/JNK signalling pathways by targeting Rab6B in human gastric cancer. *Cancer Gene Ther.* **2020**;27(6):461–472.
- [13] Santos-Faria J, Gavina C, Rodrigues P, et al. MicroRNAs and ventricular remodeling in aortic stenosis. *Rev port cardiol.* **2020**;39(7):377–387.
- [14] Santos-Faria J, Gavina C, Rodrigues P, et al. MicroRNAs and ventricular remodeling in aortic stenosis. *Rev port cardiol: orgao oficial da Sociedade Portuguesa de Cardiologia = Portuguese j cardiol: off j Portuguese Soc Cardiol.* **2020**;39(7):377–387.
- [15] Luo M, Ding L, Li Q, et al. miR-668 enhances the radioresistance of human breast cancer cell by targeting IκBa. *Breast Cancer (Tokyo, Japan).* **2017**;24(5):673–682.
- [16] Lin J, Fan X, Chen J, et al. Small interfering RNA-mediated knockdown of KRT80 suppresses colorectal cancer proliferation. *Exp Ther Med.* **2020**;20(6):176.
- [17] Toivola DM, Boor P, Alam C, et al. Keratins in health and disease. *Curr Opin Cell Biol.* **2015**;32:73–81.
- [18] Omary MB, Ku NO, Strnad P, et al. Toward unraveling the complexity of simple epithelial keratins in human disease. *J Clin Invest.* **2009**;119(7):1794–1805.
- [19] Liu O, Wang C, Wang S, et al. Keratin 80 regulated by miR-206/ETS1 promotes tumor progression via the MEK/ERK pathway in ovarian cancer. *J Cancer.* **2021**;12(22):6835–6850.
- [20] Perone Y, Farrugia AJ, Rodríguez-Meira A, et al. SREBP1 drives keratin-80-dependent cytoskeletal changes and invasive behavior in endocrine-resistant ERα breast cancer. *Nat Commun.* **2019**;10(1):2115.
- [21] Song H, Xu Y, Xu T, et al. CircPIP5K1A activates KRT80 and PI3K/AKT pathway to promote gastric cancer development through sponging miR-671-5p. *Biomed Pharmacother.* **2020**;126:109941.
- [22] Fang J, Wang H, Liu Y, et al. High KRT8 expression promotes tumor progression and metastasis of gastric cancer. *Cancer Sci.* **2017**;108(2):178–186.
- [23] Wang PB, Chen Y, Ding GR, et al. Keratin 18 induces proliferation, migration, and invasion in gastric cancer via the MAPK signalling pathway. *Clin Exp Pharmacol Physiol.* **2020**;48(1):147–156.
- [24] Pai SI, Lin YY, Macaes B, et al. Prospects of RNA interference therapy for cancer. *Gene Ther.* **2006**;13(6):464–477.
- [25] Ahadi A. A systematic review of microRNAs as potential biomarkers for diagnosis and prognosis of gastric cancer. *Immunogenetics.* **2021**;73(2):155–161.
- [26] Ouyang J, Xie Z, Lei X, et al. Clinical crosstalk between microRNAs and gastric cancer (review). *Int J Oncol.* **2021**;58(4). DOI:10.3892/ijo.2021.5187.
- [27] Wang H, Sun G, Xu P, et al. Circular RNA TMEM87A promotes cell proliferation and metastasis of gastric cancer by elevating ULK1 via sponging miR-142-5p. *J Gastroenterol.* **2020**;56(2):125–138.
- [28] Li J, Ye D, Shen P, et al. Mir-20a-5p induced WTX deficiency promotes gastric cancer progressions through regulating PI3K/AKT signaling pathway. *J Exp Clin Cancer Res.* **2020**;39(1):212.
- [29] Bertoli G, Cava C, Castiglioni I. MicroRNAs: new biomarkers for diagnosis, prognosis, therapy prediction and therapeutic tools for breast cancer. *Theranostics.* **2015**;5(10):1122–1143.